GEOPHYSICAL RESEARCH LETTERS, VOL. 36, L19301, doi:10.1029/2009GL040006, 2009

Bottom pressure signals at the TAG deep-sea hydrothermal field: Evidence for short-period, flow-induced ground deformation

Robert A. Sohn,[1] Richard E. Thomson,[2] Alexander B. Rabinovich,[2,3] and Steven F. Mihaly[2]

Received 10 July 2009; revised 19 August 2009; accepted 1 September 2009; published 1 October 2009.

[1] Bottom pressure measurements acquired from the TAG hydrothermal field on the Mid-Atlantic Ridge (26°N) contain clusters of narrowband spectral peaks centered at periods from 22 to 53.2 minutes. The strongest signal at 53.2 min corresponds to 13 mm of water depth variation. Smaller, but statistically significant, signals were also observed at periods of 22, 26.5, 33.4, and 37.7 min (1–4 mm amplitude). These kinds of signals have not previously been observed in the ocean, and they appear to represent vertical motion of the seafloor in response to hydrothermal flow - similar in many ways to periodic terrestrial geysers. We demonstrate that displacements of 13 mm can be produced by relatively small flow-induced pressures (several kPa) if the source region is less than ~100 m below the seafloor. We suggest that the periodic nature of the signals results from a non-linear relationship between fluid pore pressure and crustal permeability. **Citation:** Sohn, R. A., R. E. Thomson, A. B. Rabinovich, and S. F. Mihaly (2009), Bottom pressure signals at the TAG deep-sea hydrothermal field: Evidence for short-period, flow-induced ground deformation, *Geophys. Res. Lett.*, *36*, L19301, doi:10.1029/2009GL040006.

1. Introduction

[2] There is growing evidence that hydrothermal flow induces ground surface displacements (GSD) in active geothermal regions [e.g., *Battaglia et al.*, 2006; *Gottsmann et al.*, 2007; *Todesco and Berrino*, 2005]. These findings provide new opportunities for the use of geodetic techniques to monitor sub-surface fluid flow and have important implications for the monitoring of volcanic calderas [e.g., *Hurwitz et al.*, 2007]. Until now, evidence for hydrothermal flow-induced GSD has been restricted to subaerial volcanic systems. Here, we present evidence for flow-induced GSD at the TAG deep-sea hydrothermal field located at 26°N on the Mid-Atlantic Ridge at water depths of ~3600 m (Figure 1).

[3] The TAG field is located on the hanging wall of an active oceanic detachment fault [e.g., *deMartin et al.*, 2007; *Rona*, 1980; *Tivey et al.*, 2003] and contains the largest known concentration of massive sulfide deposits on the deep seafloor [e.g., *Humphris and Cann*, 2000; *Rona et al.*, 1993]. Known high-temperature discharge at TAG is restricted to the 'active' mound, which discharges fluids with temperatures of up to ~360°C [*Sohn*, 2007], at rates of order 1 GW [*Wichers et al.*, 2005]. The active mound is a multi-tiered, circular, mineral deposit roughly the size of a large sporting stadium (~200 m diameter, ~60 m tall). The TAG field also contains the weakly discharging 'Shimmering Mound' [*Rona et al.*, 1998], as well as more than a dozen inactive high-temperature sulfide deposits spread over an area of at least 5 km × 3 km (Figure 1), and representing more than 100,000 years of high-temperature discharge [*Lalou et al.*, 1998].

2. Experimental Methods and Observations

[4] In July 2003, we used *DSRV Alvin* to deploy a deep-sea pressure gauge (*Seabird* SBE26 Wave and Tide Gauge) in a plastic (Extren) frame at a site ~350 m northwest of the active TAG mound (Figure 2a) as part of the Seismicity and Fluid Flow of TAG (STAG) experiment. The instrument measured pressure and temperature every 10 minutes for 6 months until January 2004. Most of the bottom pressure signal is due to diurnal, semi-diurnal, and higher frequency sea surface tidal displacements (e.g., the K_1, O_1, M_2, S_2, MK_3, and M_4 tidal constituents) [*Foreman*, 1977] and large-scale, possibly topographically-amplified, barotropic motions within the 2–10 day "weather band" [*Cannon and Thomson*, 1996]. However, spectral analysis also reveals the presence of clusters of narrow-band oscillations centered on periods ranging from 22 to 53 minutes (Figure 2b). These short-period pressure oscillations are not instrumentation artifacts and were not observed, for example, in a deployment of the same gauge near a hydrothermal field on the East Pacific Rise, 9°50′N (Figure 2c). Although the relatively long sampling rate (10 min) fails to render the displacement cycles in detail, the narrow-band peaks clearly require a highly regular source process. Multiple filter analysis [*Emery and Thomson*, 2001] confirms that the peak oscillations seen in the spectrum at 53.2 min period persisted throughout the entire observational period (see auxiliary material).[4] Deep-sea pressure variations may result from either vertical displacement of the seafloor (i.e., geological processes), or thickness variations in the overlying water column (i.e., oceanographic processes). However, as there is no known oceanographic explanation for these persistent, narrow-band, short-period signals, we conclude that they represent vertical deformation of the seafloor.

3. Source Model

[5] There are no crustal magma bodies beneath the hydrothermal field [*Canales et al.*, 2007], which allows us

[1]Woods Hole Oceanographic Institution, Woods Hole, Massachusetts, USA.
[2]Department of Fisheries and Oceans, Institute of Ocean Sciences, Sidney, British Columbia, Canada.
[3]Shirshov Institute of Oceanology, Moscow, Russia.

0094-8276/09/2009GL040006$05.00

[4]Auxiliary materials are available in the HTML. doi:10.1029/2009GL040006.

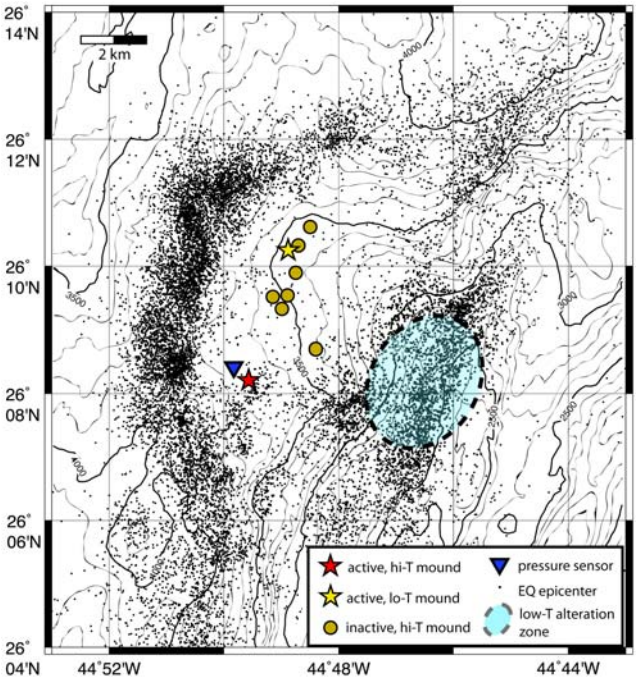

Figure 1. Bathymetric map (100 m contours) of the TAG hydrothermal field, including microearthquake epicenters delineating sub-surface position of major fault systems hosting fluid flow [*deMartin et al.*, 2007]. Known deposits include the active TAG (high-temperature) and Shimmering (low-temperature) mounds, and several relict (inactive) mounds. The broad zone of low-grade alteration observed by *Rona et al.* [1984] is also shown. The seafloor position of the bottom pressure measurements ~350 m from the active TAG mound is shown with a blue triangle.

to rule out magmatic sources as feasible mechanisms. Nonvolcanic fault tremor has characteristic frequencies of a few Hz [e.g., *Nadeau and Dolenc*, 2005; *Obara*, 2002; *Rogers and Dragert*, 2003], which are too high to explain our observed signals. The signal periods appear to be forced directly by the source mechanism because they are too long to represent resonant modes of elastic structures associated with the detachment fault (i.e., the hanging wall and/or the foot wall), which would have minimum modal periods of

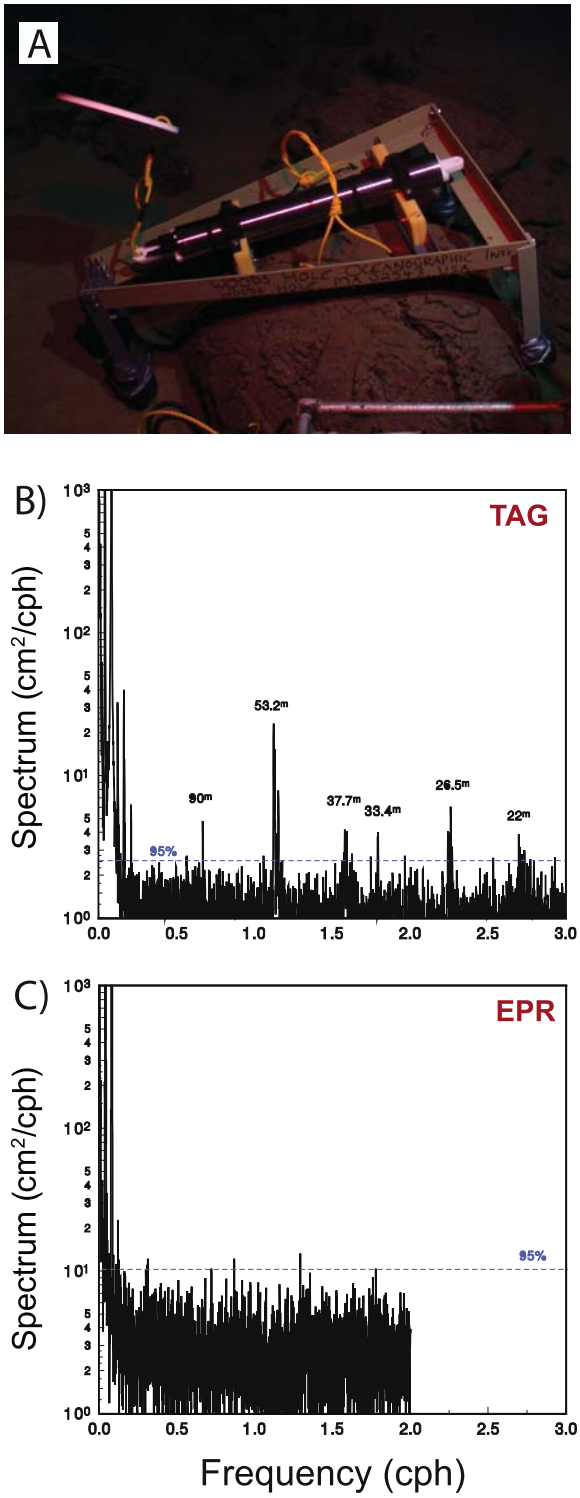

Figure 2. Bottom pressure data. (a) Digital image (acquired from *DSRV Alvin*) of *SeaBird* SBE 26 Wave and Tide Gauge deployed in the TAG hydrothermal field. The gauge was mounted in an Extren plastic frame including a rope 'handle' for the robotic manipulator arm and a white bucket lid with reflective tape to aid in locating the gauge for recovery; (b) spectrum for 10-min seafloor pressure time series data collected from the TAG hydrothermal field from 26 June 2003 to 15 January 2004. Superscript "m" denotes peak periods in minutes. Pressure has been converted to sea level height using the conversion 1 hPa ~ 1 cm. The records have a total length $NT = 29290$ (203.403 days) and spectral estimates are determined using a moving Kaiser-Bessel window of length $N = 4096$ (28.5 days) with 50% overlap, for a total of 26 degrees of freedom per spectral band [cf., *Emery and Thomson*, 2001]. Frequency (in cycles per hour, cph) is plotted on a linear scale to better show the short-period spectral peaks; and (c) same as Figure 2b but for 15-min seafloor pressure time series data collected with the same gauge from the East Pacific Rise hydrothermal field at 9°50′N from 24 April 2006 to 14 January 2007 [*Carbotte et al.*, 2004] (www.marine-geo.org/ridge2000). The data are plotted on the same axes as those used for the TAG records to facilitate direct comparisons, but the Nyquist frequency is slightly lower owing to the slower sampling rate (15 vs. 10 min intervals). No short-period pressure signals are observed in this dataset.

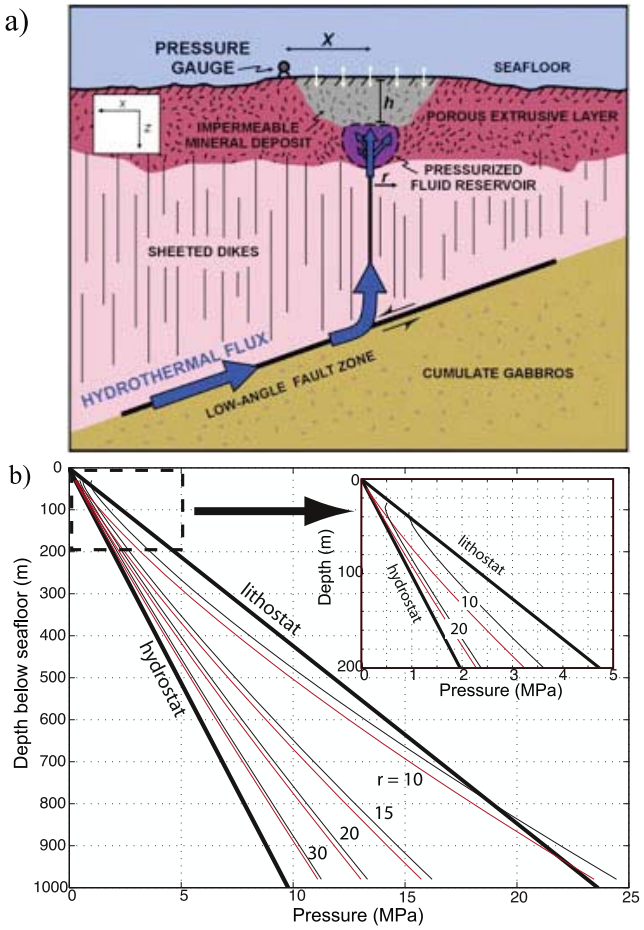

Figure 3. Ground displacement model. (a) Model schematic (see Table S1 for parameter values). (b) Model results showing the pressure, *P*, required to produce 13 mm peak-to-peak vertical ground surface displacement. The required pressure is a function of the depth of the source below the seafloor (*h*) the area (i.e., radius, *r* in meters) of the over-pressured region, and the distance of the source from the measurement location (*x*). Separate curves are shown for source radii ranging from 10 to 30 m. Red curves show pressure required if source is directly below the sensor ($x = 0$). Black curves show pressure required if source is directly beneath the active mound (x = 350 m). Inset panel shows zoom of upper 200 m.

order a few Hz assuming the elastic parameters given in Table S1, and maximum length scales of a few tens of kilometers [e.g., *Gorman*, 1978]. The spectral peak at 53.2 min is not associated with the ${}_0S_2$ eigen-oscillation of the Earth because the frequency is slightly too high - 313.28 vs. 309.45 ± 0.15 μHz [*Masters and Widmer*, 1995] - and because the oscillations are continuous over the entire six-month recording interval and, therefore, not associated with strong earthquakes, the usual source of episodic Earth oscillations. Hydrothermal flow appears to be the only geological process capable of explaining the amplitude and period of the inferred ground displacement signal.

[6] Although hydrothermal flow-induced GSD has not previously been documented on the deep seafloor, fluid/heat flux rate estimates for the active TAG mound range from 100 MW to ~1 GW [*Kinoshita et al.*, 1998; *Wichers et al.*, 2005], which are similar to, and possibly an order of magnitude larger than, geothermal fields on land where flow-induced GSD has been documented and/or proposed [e.g., *Chiodini et al.*, 2001]. The deformation displacements we observed (≤13 mm) are modest compared to observations and models for subaerial geothermal fields [e.g., *De Natale et al.*, 2001; *Hutnak et al.*, 2009], and the cycle periods are similar to many geyser eruption intervals, which are typically 10s of minutes up to several hours, and which can be associated with systematic inflation/deflation GSD cycles [*Nishimura et al.*, 2006]. The strict analogy to geysers is probably limited by the fact that the volume expansion associated with phase transitions is ~500 times smaller in the deep-sea environment at TAG compared to subaerial geothermal fields [e.g., *Driesner*, 2007], but the concept of highly-regular pressure cycles associated with the steady flux of fluid and heat into a sub-surface reservoir appears to provide the most likely explanation for our observations.

[7] We consider the response of a thin, elastic shell to a static point load, *P*, to determine the first-order feasibility of the proposed source mechanism. The vertical displacement, *w*, of the shell is given by

$$w(r) = \left(\frac{P\beta^2}{2\pi D}\right) kei\left(\frac{r}{\beta}\right)$$

where *r* is the radius (distance) from the point load, β and *D* are, respectively, the 3-dimensional flexural parameter and rigidity of the elastic plate, and *kei* is a zero-order Bessel-Kelvin function [*Brotchie and Silvester*, 1969; *Watts*, 2001]. The flexural parameter and rigidity are functions of the intrinsic mechanical properties of the elastic plate and its thickness, *h*, such that:

$$D = \frac{Eh^3}{12(1-\nu^2)}, \beta = \left[\frac{D}{\Delta\rho g}\right]^{1/4}$$

where *E* is Young's modulus, ν is Poisson's ratio, $\Delta\rho$ is the density difference between the elastic plate and the underlying substrate, and *g* is the acceleration of gravity. Mechanical parameter values appropriate for shallow oceanic crust are shown in Table S1.

[8] Figure 3a presents a schematic of our simple model. The vertical GSD generated by pressurization of a sub-surface fluid reservoir is primarily a function of the magnitude and depth of the point load, the elastic parameters of the overlying crust, and lateral offset distance of the measurement from the source. The offset distance from the pressure source is unknown, but we consider two possibilities; (1) the end-member case where the source is immediately below our measurement site (i.e., x = 0), and (2) a more likely case where the source is beneath the active TAG mound (i.e., x = 350 m), the only presently known site of high-temperature discharge. For these two cases, we can then estimate the magnitude of the load, *P*, required to produce 13 mm of peak-to-peak vertical displacement (the mean amplitude signal at 53.2 min period) as a function of source depth. We assume that the background reservoir

pressure is in hydrostatic equilibrium, and then determine how much excess pressure is required to produce the observed 13 mm ground displacement signal.

[9] Figure 3 shows the point load required to produce 13 mm of ground displacement as a function of depth from the seafloor down ~1 km to the detachment fault underlying the hydrothermal field [*Canales et al.*, 2007]. For the range of reservoir size we examined, the required source size is a strong function of depth. Relatively small overpressures (several kPa to ~1 MPa above hydrostatic) are required if the reservoir is located in the shallow crust (upper hundred meters), as shown in the inset to Figure 3, but somewhat larger overpressures (several MPa) are required if the reservoir is located on or near the detachment fault.

4. Discussion

[10] In principle, the pressure cycles we observed could be caused by either seafloor displacements or changes in the thickness of the overlying water column, but there are no oceanographic processes we can put forward that would produce these kinds of persistent, high-frequency, narrow-band signals. Tilt cycles with similar periods have been observed near the Logatchev hydrothermal field on the MAR at 14°45′N [*Fabian and Villinger*, 2008], and when combined with our bottom pressure data, these observations provide compelling evidence for regular, hydrothermal flow-induced, GSD cycles at deep-sea hydrothermal fields.

[11] The primary characteristics of our pressure data are; (1) the cyclic displacements (4 to 13 mm), (2) the highly-regular period of the cycles (22 to 53 minutes), and (3) the presence of multiple clusters of spectral peaks. We have shown that the signal amplitudes can be produced to first-order with relatively small overpressures (order kPa) in a shallow sub-surface fluid reservoir, or alternatively, fluid overpressures of several MPa in a deeper reservoir. Fluid pressure levels in deep-sea hydrothermal flow systems are not well-understood, but there is ample evidence that fluid pressures may reach, or even exceed, lithostatic levels in some fault systems (e.g., subduction and metamorphic fault zones [*Sibson and Scott*, 1998; *Sibson*, 2007]). On this basis, we conclude that the source regions could be anywhere on or above the detachment fault underlying the hydrothermal field.

[12] Subaerial geysers generate regular GSD cycles with periods of order tens of minutes [*Nishimura et al.*, 2006], and while our sampling rate was not fast enough to allow for direct comparisons of our pressure signal with the sawtooth tilt patterns observed for geysers, the highly-regular, cyclical nature of our signal is suggestive of geyser processes. Geyser eruptions are often attributed to the volume expansion associated with phase transitions during reservoir decompression [e.g., *Ingebritsen and Rojstaczer*, 1993], and the viability of this feedback mechanism at the super-critical pressures of the TAG field is not known. Another possibility is that fluid pore pressures and permeability are coupled in the shallow crust, which could also introduce non-linear, periodic, behavior into the flow system. The presence of multiple spectral peaks in the 20–50 min period range implies the existence of multiple sub-surface pressure sources, since the elastic resonant modes of the crust are at much shorter periods. This in turn implies that there are a number of fluid sub-reservoirs distributed beneath the hydrothermal field, but more comprehensive seafloor geodetic surveys will be needed to determine the nature and spatial distribution of the source mechanisms driving the short-period GSD cycles we observed at TAG.

[13] **Acknowledgments.** The authors would like to thank Dan Fornari and the WHOI Deep Submergence Facility for assistance with deployment of the tide gauge, Patricia Kimber for assisting with the figures, and Shaul Hurwitz and two anonymous reviewers for helpful reviews of the manuscript.

References

Battaglia, M., et al. (2006), Evidence for fluid migration as the source of deformation at Campi Flegrei caldera (Italy), *Geophys. Res. Lett.*, *33*, L01307, doi:10.1029/2005GL024904.

Brotchie, J. F., and R. Silvester (1969), On crustal flexure, *J. Geophys. Res.*, *74*, 5240–5245, doi:10.1029/JB074i022p05240.

Canales, J. P., R. A. Sohn, and B. J. deMartin (2007), Crustal structure of the Trans-Atlantic Geotraverse (TAG) segment (Mid-Atlantic Ridge, 26(10′N): Implications for the nature of hydrothermal circulation and detachment faulting at slow spreading ridges, *Geochem. Geophys. Geosyst.*, *8*, Q08004, doi:10.1029/2007GC001629.

Cannon, G. A., and R. E. Thomson (1996), Characteristics of a 4-day oscillation trapped by the Juan de Fuca Ridge, *Geophys. Res. Lett.*, *23*, 1613–1616, doi:10.1029/96GL01370.

Carbotte, S. M. (2004), New integrated data management system for Ridge2000 and MARGINS research, *Eos Trans. AGU*, *85*(51), doi:10.1029/2004EO510002.

Chiodini, G., et al. (2001), CO_2 degassing and energy release at Solfatara volcano, Campi Flegrei, Italy, *J. Geophys. Res.*, *106*, 16,213–216,221, doi:10.1029/2001JB000246.

De Natale, G., et al. (2001), A mechanical fluid-dynamical model for ground movements at Campi Flegrei caldera, *J. Geodyn.*, *32*, 487–517, doi:10.1016/S0264-3707(01)00045-X.

deMartin, B., et al. (2007), Kinematics and geometry of active detachment faulting beneath the Trans-Atlantic Geotraverse (TAG) hydrothermal field on the Mid-Atlantic Ridge, *Geology*, *35*, 711–714, doi:10.1130/G23718A.1.

Driesner, T. (2007), The system H_2O-NaCl, Part II: Correlations for molar volume, enthalpy, and isobaric heat capacity from 0 to 1000°C, 1 to 5000 bar, and 0 to 1 X_{NaCl}, *Geochim. Cosmochim. Acta*, *71*, 4902–4919, doi:10.1016/j.gca.2007.05.026.

Emery, W. J., and R. E. Thomson (2001), *Data Analysis Methods in Physical Oceanography*, 2nd ed., 638 pp., Elsevier Sci., New York.

Fabian, M., and H. Villinger (2008), Long-term tilt and acceleration data from the Logatchev Hydrothermal Vent Field, Mid-Atlantic Ridge, measured by the Bremen Ocean Bottom Tiltmeter, *Geochem. Geophys. Geosyst.*, *9*, Q07016, doi:10.1029/2007GC001917.

Foreman, M. G. G. (1977), *Manual for Tidal Height Analysis and Prediction*, Inst. of Ocean Sci., Sidney, B. C., Canada.

Gorman, D. J. (1978), Free vibration analysis of the completely free rectangular plate by the method of superposition, *J. Sound Vibrat.*, *57*(3), 437–447, doi:10.1016/0022-460X(78)90322-X.

Gottsmann, J., R. Carniel, N. Coppo, L. Wooller, S. Hautmann, and H. Rymer (2007), Oscillations in hydrothermal systems as a source of periodic unrest at caldera volcanoes: Multiparameter insights from Nisyros, Greece, *Geophys. Res. Lett.*, *34*, L07307, doi:10.1029/2007GL029594.

Humphris, S. E., and J. R. Cann (2000), Constraints on the energy and chemical balances of the modern TAG and ancient Cyprus seafloor sulfide deposits, *J. Geophys. Res.*, *105*, 28,477–28,488, doi:10.1029/2000JB900289.

Hurwitz, S., L. B. Christiansen, and P. A. Hsieh (2007), Hydrothermal fluid flow and deformation in large calderas: Inferences from numerical simulations, *J. Geophys. Res.*, *112*, B02206, doi:10.1029/2006JB004689.

Hutnak, M., S. Hurwitz, S. E. Ingebritsen, and P. A. Hsieh (2009), Numerical models of caldera deformation: Effects of multiphase and multicomponent hydrothermal fluid flow, *J. Geophys. Res.*, *114*, B04411, doi:10.1029/2008JB006151.

Ingebritsen, S. E., and S. A. Rojstaczer (1993), Controls on geyser periodicity, *Science*, *262*, 889–892, doi:10.1126/science.262.5135.889.

Kinoshita, M., et al. (1998), Tidally-driven effluent detected by long-term temperature monitoring at the TAG hydrothermal mound, Mid-Atlantic Ridge, *Phys. Earth Planet. Inter.*, *108*, 143–154, doi:10.1016/S0031-9201(98)00092-2.

Lalou, C., et al. (1998), Age of sub-bottom sulfide samples at the TAG active mound, in *Proceedings of Ocean Drilling Program, Scientific Results*, edited by P. M. Herzig et al., pp. 111–117, Ocean Drill. Program, College Station, Tex.

Masters, T. G., and R. Widmer (1995), Free oscillations, frequencies, and attenuations, in *Global Earth Physics: A Handbook of Physical Constants*, edited by T. J. Ahrens, pp. 104–125, AGU, Washington, D. C.

Nadeau, R. M., and D. Dolenc (2005), Nonvolcanic tremors deep beneath the San Andreas Fault, *Science*, *307*, 389, doi:10.1126/science.1107142.

Nishimura, T., et al. (2006), Investigation of the Onikobe geyser, NE Japan, by observing the ground tilt and flow parameters, *Earth Planets Space*, *58*, e21–e24.

Obara, K. (2002), Nonvolcanic deep tremor associated with subduction in southwest Japan, *Science*, *296*, 1679–1681, doi:10.1126/science.1070378.

Rogers, G., and H. Dragert (2003), Episodic tremor and slip on the Cascadia Subductioni Zone: The chatter of silent slip, *Science*, *300*, 1942–1943, doi:10.1126/science.1084783.

Rona, P. A. (1980), TAG hydrothermal field: Mid-Atlantic Ridge crest at latitude 26°N, *J. Geol. Soc.*, *137*, 385–402, doi:10.1144/gsjgs.137.4.0385.

Rona, P. A., et al. (1984), Hydrothermal activity at the TAG hydrothermal field, Mid-Atlantic Ridge crest at 26°N, *J. Geophys. Res.*, *89*, 11,365–11,377, doi:10.1029/JB089iB13p11365.

Rona, P. A., et al. (1993), Active and relict seafloor hydrothermal mineralization at the TAG hydrothermal field, Mid-Atlantic Ridge, *Econ. Geol.*, *88*, 1989–2017, doi:10.2113/gsecongeo.88.8.1989.

Rona, P. A., et al. (1998), An active, low temperature hydrothermal mound and a large inactive sulfide mound found in the TAG hydrothermal field, Mid-Atlantic Ridge 26N, 45W, *Eos Trans. AGU*, *79*, F920.

Sibson, R. H. (2007), An episode of fault-valve behavior during compressional inversion?—The 2004 Mj6.8 Mid-Niigata Prefecture, Japan, earthquake sequence, *Earth Planet. Sci. Lett.*, *257*, 188–199, doi:10.1016/j.epsl.2007.02.031.

Sibson, R. H., and J. Scott (1998), Stress/fault controls on the containment and release of overpressured fluids: Examples from gold-quartz veins in Juneau, Alaska; Victoria, Australia, and Otago, New Zealand, *Ore Geol. Rev.*, *13*, 293–306, doi:10.1016/S0169-1368(97)00023-1.

Sohn, R. A. (2007), Stochastic analysis of exit fluid temperature records from the active TAG hydrothermal mound (Mid-Atlantic Ridge, 26°N): 1. Modes of variability and implications for subsurface flow, *J. Geophys. Res.*, *112*, B07101, doi:10.1029/2006JB004435.

Tivey, M. A., H. Schouten, and M. C. Kleinrock (2003), A near-bottom magnetic survey of the Mid-Atlantic Ridge axis at 26°N: Implications for the tectonic evolution of the TAG segment, *J. Geophys. Res.*, *108*(B5), 2277, doi:10.1029/2002JB001967.

Todesco, M., and G. Berrino (2005), Modeling hydrothermal fluid circulation and gravity at the Phlegraean Fields caldera, *Earth Planet. Sci. Lett.*, *240*, 328–338, doi:10.1016/j.epsl.2005.09.016.

Watts, A. B. (2001), *Isostasy and Flexure of the Lithosphere*, 458 pp., Cambridge Univ. Press, Cambridge, U. K.

Wichers, S., et al. (2005), New constraints on the thermal power of the TAG hydrothermal system and the dynamics of the water column plume, *Eos Trans. AGU*, *86*(52), Fall Meet. Suppl., Abstract OS33A-1466.

S. F. Mihaly, A. B. Rabinovich, and R. E. Thomson, Department of Fisheries and Oceans, Institute of Ocean Sciences, P.O. Box 6000, Sidney, BC V8L 4B2, Canada.

R. A. Sohn, Woods Hole Oceanographic Institution, MS 24, 360 Woods Hole Road, Woods Hole, MA 02543, USA. (rsohn@whoi.edu)